

Experimental validation of the design and control of a compressed air energy storage system

Ilham Rais¹, Chafik Ed-dahmani², Abdellah Benami³

¹Power Electronics and Control Laboratory, Department of Electrical Engineering, Mohamadia School of Engineering, Mohammed V University, Rabat, Morocco

²Engineering Sciences and Professions Laboratory, National Graduate School of Arts and Crafts, Moulay Ismail University, Meknes, Morocco

³Optoelectrics and Applied Energy Techniques, Department of Physics, Faculty of Sciences and Techniques, Moulay ismail University of Meknes, Errachidia, Morocco

Article Info

Article history:

Received Jan 16, 2024

Revised Jul 13, 2024

Accepted Jul 24, 2024

Keywords:

Boost converter

Compressed air energy storage

Incremental conductance

MPPT

Perturb and observe

ABSTRACT

In this paper, we introduce a comprehensive design and control strategy for an energy storage system based on compressed air to enhance both electrical energy quality and operational flexibility. The formulation of this control structure involved extensive calculations and computer simulations, which now require experimental validation. We describe the specifically designed test benches for this purpose and present an analysis of the experimental results. The paper begins with a brief overview of the didactic bench used to test the pure pneumatic conversion system, followed by the presentation and discussion of the initial practical results of the maximum energy point tracking (MEPT) strategy derived from this bench.

This is an open access article under the [CC BY-SA](https://creativecommons.org/licenses/by-sa/4.0/) license.



Corresponding Author:

Ilham Rais

Power Electronics and Control Laboratory, Department of Electrical Engineering

Mohamadia School of Engineering, Mohammed V University

Rabat, Morocco

Email: ilhamrais@research.emi.ac.ma

1. INTRODUCTION

In the majority of remote locales, the primary source of electrical power is typically represented by diesel generators. Within these particular regions, the cost associated with expanding the conventional electricity grid is deemed prohibitive, further compounded by the significant escalation in fuel prices due to the isolation factor [1]. The sustained decrease in the cost of renewable energy-based generator systems, along with the steadily improving dependability of these technologies, has facilitated a heightened adoption of renewable energy sources for electricity generation within remote regions [2], [3].

In Morocco, as an illustrative case, alongside the burgeoning adoption of wind and solar energy, primarily through the establishment of large-scale facilities integrated with centralized distribution networks, the provision of electricity to remote locations through diesel generators continues to present considerable technical and financial challenges [4], [5]. This method of electricity generation is characterized by its inherent inefficiency, exorbitant cost, and substantial greenhouse gas (GHG) emissions [3], [6].

The combination of wind and solar (joint energy systems (JES)) within these self-contained networks shows promise for alleviating operational deficiencies. Nevertheless, the economic sustainability of JES rests on reaching a large penetration rate of wind or solar energy, a feat feasible only through the deployment of

energy storage systems. In this work, a comprehensive solution is provided that matches with both technical and budgetary demands, enabling the dependable distribution of electricity to remote places.

This concept comprises the development of a hybrid wind-photovoltaic system equipped with compressed air storage. Hence, revolutionary concepts in compressed air energy storage (CAES) have recently developed, establishing CAES as an appealing storage technology for the seamless integration of renewable energy sources into the power grid [2], [7], [8]. As a notable development, small-scale compressed air energy storage (SSCAES) systems have been created, with a focus on their implementation in rural areas and developing countries [9], [10]. Air is stored in tanks or containers in these small systems [2], [11].

The compressed air is then used to power an air motor or turbine, which in turn moves an electric generator that generates power for users. The charging and discharging procedures of SS-CAES entirely rely on clean air as an energy source, making it an attractive alternative for usage with renewable energy sources [1], [12], [13]. Comparing SS-CAES to more widely recognized energy storage devices, such as lithium batteries [10], it becomes evident that SS-CAES exhibits lower energy density. However, it is important to note that batteries generate toxic waste and are susceptible to potential overheating and explosions arising from their internal resistance. Consequently, the implementation of a battery management system is imperative for their safe operation [14], [15].

In this study, as illustrated in Figure 1 the pneumatic-to-electrical conversion process can be reduced into two independent processes. Firstly, mechanical energy is generated by the employment of an air motor. Subsequently, the mechanical energy is further turned into electrical energy via a standard direct current (DC) machine. It is vital to note that this research primarily focuses on the discharge process, and as such, it includes the employment of a tiny DC generator. This technique provides an easy and speedy control of the electro-mechanical conversion process [2], [16]. To manage and regulate the system's operation and attain the desired output power conditioning, a Buck converter is employed in this paper.

The algorithm used in this paper is capable of ensuring the correct direction of speed adjustments in response to transient fluctuations in input power. The system's behavior is analyzed through the utilization of a small signal model. A digital speed regulator is specifically engineered to manage the output power of the DC generator, thereby achieving the targeted maximum power point tracking (MPPT). Subsequently, the MPPT algorithm is subjected to simulation and experimental implementation.

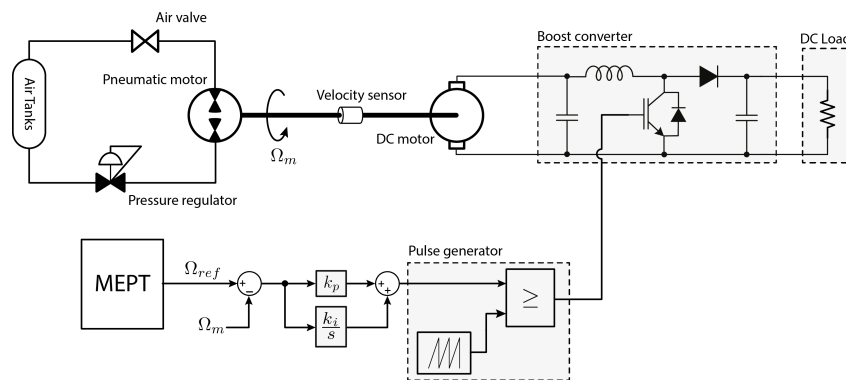


Figure 1. Pneumatic energy conversion principle using volumetric air machine

2. MAXIMUM POWER POINT TRACKING STRATEGY IMPLEMENTATION FOR THE STUDIED SYSTEM

The work presented in [17] highlights the power characteristics of the compressed air motor [1], [18], [19]. The analysis reveals the existence of a critical operational point where maximum power output is achieved. This maximum power output is crucial, particularly during peak demand scenarios, underscoring the necessity for precise control of the motor's speed to ensure optimal power delivery [2], [5]. Various maximum power point tracking (MPPT) monitoring strategies have been proposed in the literature, including methods such as perturb and observe (PO), incremental conductance (IC), and fuzzy logic, among others [20], [21].

In this article, we apply the incremental conductance (CI) technique to track the greatest power point. This approach relies on the observation that the power curve of the pneumatic motor shows a zero slope at the

maximum power point (MPP), with increasing slopes to the left and decreasing slopes to the right [2], [3]. This relationship can be expressed as in (1).

$$P = \frac{\pi}{30}(MN) = M_1N \quad (1)$$

With: P: power of pneumatic motor; M: torque of pneumatic motor; and N: mechanical rotational speed of pneumatic motor. Thus, it can be inferred as in (2) that if:

$$\frac{dP}{dN} = \frac{M_1N}{dN} = M_1 + N \frac{dM_1}{dN} \quad (2)$$

$\frac{\Delta M_1}{\Delta N} = \frac{M_1}{N}$ The actual point is the MPP.

$\frac{\Delta M_1}{\Delta N} < \frac{M_1}{N}$ The actual point is on the left of the MPP.

$\frac{\Delta M_1}{\Delta N} > \frac{M_1}{N}$ The actual point is on the right of the MPP. The MPP can be identified by comparing the

instantaneous conductance with the incremental conductance (IC), as illustrated in the flowchart in Figure 2.

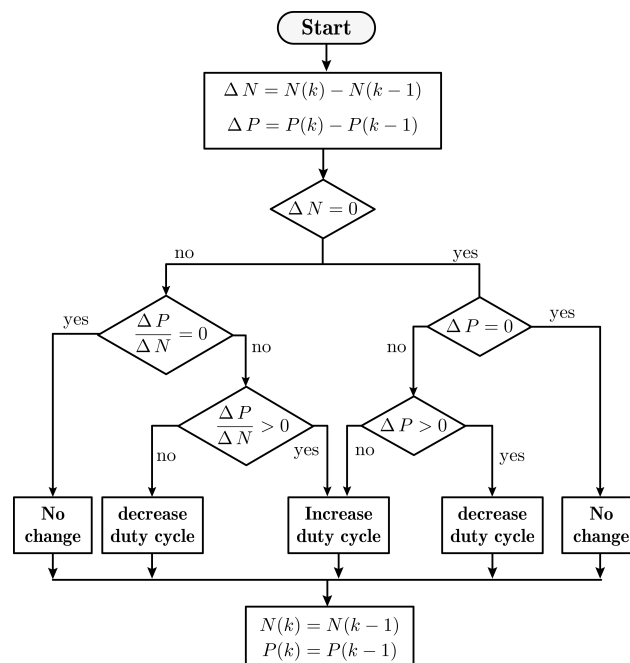


Figure 2. Incremental conductance algorithm

2.1. MPPT strategy simulation results

The provided Figure 3 depicts the theoretical outcomes of simulations conducted using MATLAB software. This graphical representation portrays the operational curve of the maximum power point tracking (MPPT) algorithm [11]. It is discernible from the graph that the analytically determined reference speed closely corresponds to the speed of the simulated motor. This alignment serves as empirical evidence supporting the efficacy and accuracy of the previously introduced MPPT algorithm [9], [10].

The discharging process demonstrates the attainment of maximum air motor power through the use of an MPPT algorithm, even amidst varying pressure conditions. The actual speed aligns with the optimal speed of the air motor, derived from the motor's maximum power as a function of pressure [22]. It is evident that the MPPT algorithm effectively facilitates a controlled reduction in speed adjustments, achieving an accuracy, while maintaining a smooth ripple speed of $t = 5s$ to optimize power conversion as the pressure transitions from 6 bar to 4 bar, and subsequently to 2 bar. Furthermore, the analysis indicates that the dynamic response of the air motor is influenced by variations in the rate of power relative to changes in both duty cycle and speed.

2.2. Dimensioning and design of the boost converter

The boost converter is a unidirectional parallel DC converter, a voltage step-up converter, consisting of an inductor L_b , a power switch (transistor), a diode, and an output capacitor C_b . It converts the input voltage V_{in} from the three-phase rectifier into an output voltage denoted as V_{out} . The conversion is achieved by controlling the transistor with a periodic signal using pulse width modulation (PWM) with a duty cycle and a frequency f_b (period: T_b) [9]-[12]. In the design phase of the boost converter, the following assumptions will be accepted: i) All components are perfect (without losses); ii) The plan will be assumed to be established; and iii) The output voltage is considered constant during the period.

After all mathematical calculation done, we denote R_{eq} as the equivalent resistance seen at the input of the converter, and R_L as the resistance seen at the output of the converter. The relationship between these two resistances can be determined by (3) [14], [23].

$$R_{eq} = (1 - \alpha)^2 R_L \quad (3)$$

The equivalent resistance R_{eq} allows adjusting the amount of power transmitted to the load R_L . It determines the current delivered by the DC generator and thus its resisting torque T_e , consequently affecting its rotational speed ω_m . The duty cycle will be adjustable to maximize the extracted power (achieved through the MPPT control) [24], [25]. The advantage of this structure lies in the simplicity of power control, as it involves a simple pulse width modulation (PWM) signal at the boost converter level, without directly controlling the DC generator [10], [20].

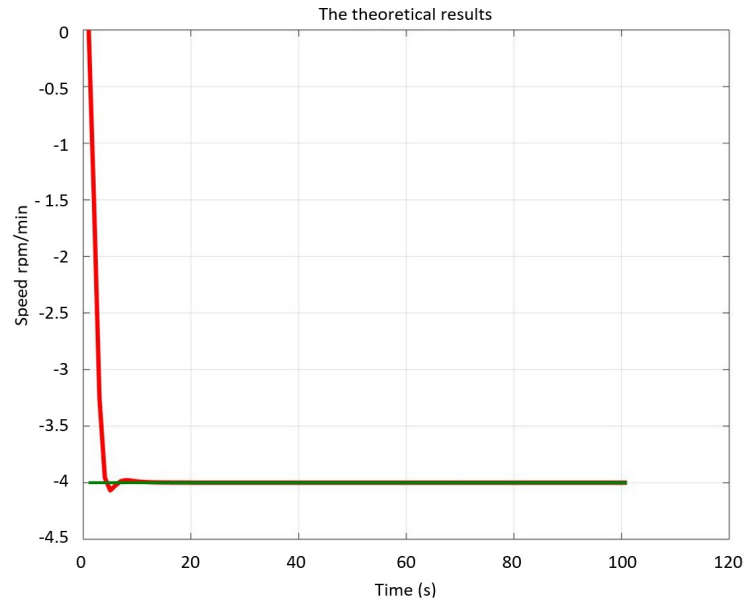


Figure 3. Theoretical results of simulation from MATLAB/Simulink

2.2.1. Determining boost converter parameter values

- Calculation of the value of the output capacitor: C_b

During phase 1, the output capacitor C_b is the only element that supplies energy to the load at the output of the boost converter. Assuming that the current is constant, the amount of charge exchanged with the load during this period, which lasts for $\alpha.T_b$, is (4) [17], [26].

$$\Delta Q = I_{out} \cdot \alpha \cdot T_b \quad (4)$$

During this period, the output voltage ripples expressed in (5).

$$\Delta V_{out} = \frac{\Delta Q}{C_b} \quad (5)$$

Then we deduce to (6).

$$C_b = \frac{I_{inv} \alpha T_b}{\Delta V_{out}} \quad (6)$$

The final form of voltage ripples is given by (7).

$$\Delta V_{out} = ESR \cdot \left(\frac{\alpha I_{inv}}{1 - \alpha} \right) + \frac{\Delta i}{2} \quad (7)$$

Here are the data for the boost converter: power: 25 W; input voltage (V_{in}): 12 V; output voltage (V_{out}): 24 V; output current (I_{out}): 1.2 A; duty cycle: 0.25; inductance (L_b): 0.1 mH; capacitor (C_b): 400 μF ; and equivalent series resistance (ESR): 270 $m\Omega$; switching frequency (f_b): 8 kHz.

- Calculation of the value of the inductor: L_b

The inductor remains the most delicate element to determine. If the inductance is over sized, it will cause significant power losses due to joule heating [22], [23]. On the other hand, if the inductance is undersized, it will act like a resistor because of its saturation. Based on (7), we find (8) [7], [27], [28].

$$L_b = \frac{\alpha V_{in}}{\Delta i \cdot f_b} \quad (8)$$

f_b : represents the frequency of the pulse width modulation (PWM) control signal of the boost converter. Figure 4 shows the experimental implementation of a boost converter with a 12V input and a 24V output.



Figure 4. Boost converter realization

3. EXPERIMENTAL RESULTS AND DISCUSSION

3.1. Test bench description

Initial experiments into the increase of pneumatic energy storage required the employment of a solely pneumatic conversion system employing a volumetric air machine. The MEPT technique was then devised to enhance the performance of this machine by including speed control. A schematic illustration of the experimental test rig built for this purpose is commented upon in the Figure 5, each number explains: i) compressed-air tank and pressure regulator, ii) compressed-air motor, iii) DC generator, iv) incremental encoder speed sensor, v) boost converter and gate driver circuit, vi) resistive load, vii) Arduino Due board, and viii) interface human-machine (PC).

The study and experimental validation employed ATLAS COPCO's LBZ14R-005 air motor, the characteristics of which were delineated in [9]. The investigation utilized compressed air sourced from a 10 bar compressed air reservoir employed as a storage apparatus, with a maximum pressure constraint of 7 bar, aligning with the recommended operational parameters for the motor. A diminutive 1 KW direct current (DC) electric machine was employed to facilitate the conversion of mechanical energy into electrical energy. The selection of a DC machine was motivated by its capacity to streamline energy conversion processes and facilitate speed regulation. For the purpose of speed control and power conditioning, a DC-DC boost converter was harnessed. The pulse width modulation (PWM) signals emitted by the Arduino Due driver board exhibited a voltage level of 0/3.3 V, while the switching transistors (MOSFETs) within the power converters necessitated logic level voltages of 0/5 V. This requisite was fulfilled through the implementation of TLP250 drivers.

3.2. Experimental results

The upcoming section will focus on the experimental validation of the maximum power point tracking (MPPT) technique, as elaborated in section 2. It is crucial to note that the functions affecting speed control

and adjustment of the DC bus voltage are executed through the Arduino Due board. Notably, the determination of airflow relies on pressure and speed measurements, applying the variable pressure model defined in (2). Likewise, mechanical torque is determined from the same set of observations, applying as (2).

Figures 6(a) and 6(b) in the presentation display the experimental plots capturing the startup behavior of the compressed air motor while operating at a constant pressure of 5 bar. It is noteworthy that the system achieves precise alignment with the setpoint value approximately one second after the initiation of the reservoir valve, primarily attributable to the utilization of the maximum power point tracking (MPPT) technique and the proportional integral (PI) control of the boost. This time delay exhibits variability due to the stochastic fluctuations in the initial torque associated with the pneumatic motor equipped with pallets within the specified configuration.

Figures 7(a) and 7(b) present the findings derived from experimental trials conducted within a dynamic pressure range spanning from 3 bar to 6 bar. In Figure 7(a), the graphical representation illustrates the presence of output voltage ripples, measuring approximately 23.7 V, primarily attributable to the influence of elevated pressures. This phenomenon is an inherent characteristic associated with the utilization of the incremental conductance (IC) technique for tracking the maximum power point (MPPT). As for the speed response, Figure 7(b) illustrates that the system attains synchronization with the predetermined setpoint signal within approximately 0.03s, it is noteworthy that this rapid response is a commendable attribute of the system.

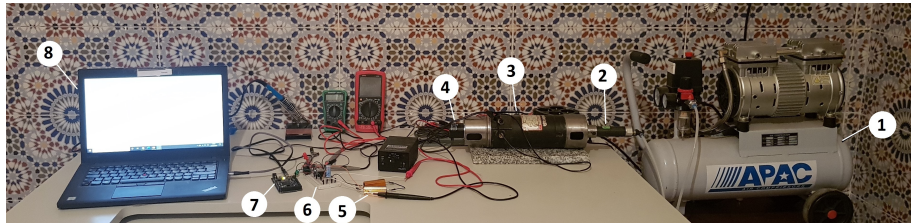


Figure 5. Experimental setup for the discharging process with MPPT algorithm

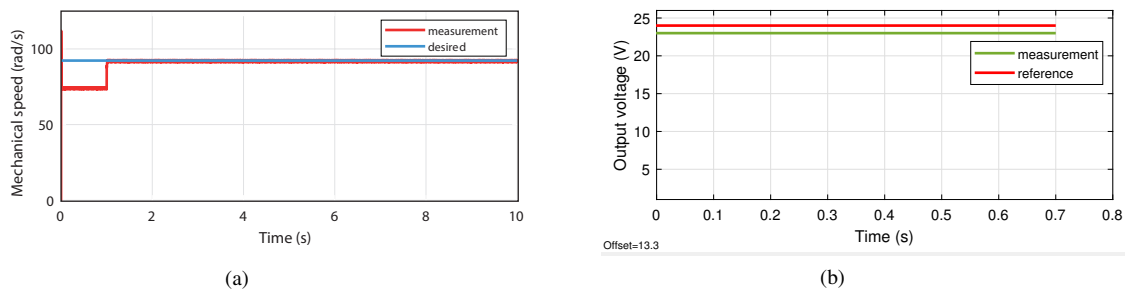


Figure 6. Experimental results: (a) variation of speed in a constant pressure system and (b) variation of voltage in a constant pressure system

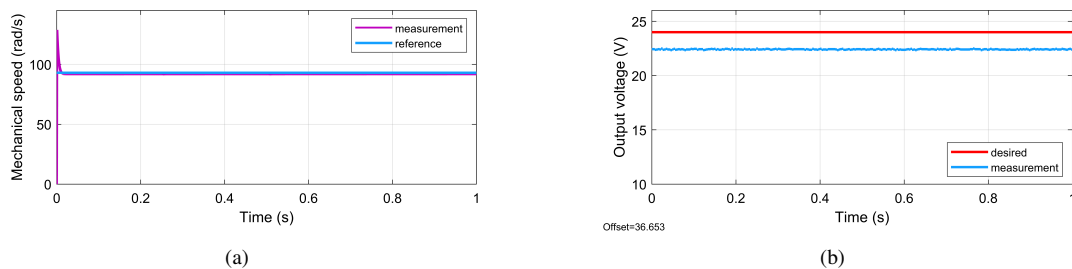


Figure 7. Experimental results: (a) variation of speed in a variable pressure system and (b) variation of voltage in a variable pressure system

The dynamic response of the system illustrated in Figure 7 demonstrates that the hybrid MPPT method incorporates a calculated speed command. Through speed regulation within the cascade proportional-integral (PI) controller, the system achieves a reference speed. The optimal speed of the air motor is analyzed based on maximum power point (MPP) considerations relative to the measured pressure. It is evident that the dynamic response of the air motor's speed corresponds closely to maximizing power output using the MPPT algorithm during the discharging process under varying pressure conditions. The convergence of the air motor's speed aligns with the characteristic air motor speed at different pressure levels corresponding to the MPP. So, we can conclude that a comparative analysis between these empirical outcomes and the simulated curves reveals a high degree of conformity, affirming the accuracy, and reliability of the implemented system.

4. CONCLUSION

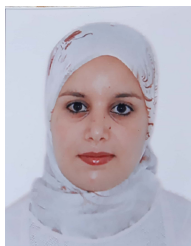
In this paper, we initiated our discourse by furnishing an exposition on the diverse constituents comprising the devised and realized test platform. Subsequently, we expounded upon the empirical substantiation of the examined algorithms employed for the extraction of the maximum power point (MPPT). The outcomes elucidated that the algorithm we proposed exhibits commendable attributes such as swift initialization and adept tracking capabilities. A comparative analysis between the empirical data and the simulated curves revealed a noteworthy concurrence between the two, affirming the robustness of our proposed algorithm.




REFERENCES

- [1] S. Huang and A. Khajepour, "A new adiabatic compressed air energy storage system based on a novel compression strategy," *Energy*, vol. 242, p. 122883, Mar. 2022, doi: 10.1016/j.energy.2021.122883.
- [2] S. Teng and H. Xi, "Experimental evaluation of vortex tube and its application in a novel trigenerative compressed air energy storage system," *Energy Conversion and Management*, vol. 268, p. 115972, Sep. 2022, doi: 10.1016/j.enconman.2022.115972.
- [3] J. Ochmann, K. Rusin, S. Rulik, S. Waniczek, and L. Bartela, "Experimental and computational analysis of packed-bed thermal energy storage tank designed for adiabatic compressed air energy storage system," *Applied Thermal Engineering*, vol. 213, p. 118750, Aug. 2022, doi: 10.1016/j.applthermaleng.2022.118750.
- [4] Q. Zhou, D. Du, C. Lu, Q. He, and W. Liu, "A review of thermal energy storage in compressed air energy storage system," *Energy*, vol. 188, p. 115993, Dec. 2019, doi: 10.1016/j.energy.2019.115993.
- [5] H. Lund and G. Salgi, "The role of compressed air energy storage (CAES) in future sustainable energy systems," *Energy Conversion and Management*, vol. 50, no. 5, pp. 1172–1179, May 2009, doi: 10.1016/j.enconman.2009.01.032.
- [6] E. Bazdar, M. Sameti, F. Nasiri, and F. Haghighat, "Compressed air energy storage in integrated energy systems: A review," *Renewable and Sustainable Energy Reviews*, vol. 167, p. 112701, Oct. 2022, doi: 10.1016/j.rser.2022.112701.
- [7] I. Rais and H. Mahmoudi, "Study and dimensioning of a compressed air storage system dedicated to the isolated site," in *2017 International Renewable and Sustainable Energy Conference (IRSEC)*, Dec. 2017, pp. 1–4, doi: 10.1109/IRSEC.2017.8477254.
- [8] Y.-M. Kim, J.-H. Lee, S.-J. Kim, and D. Favrat, "Potential and evolution of compressed air energy storage: Energy and exergy analyses," *Entropy*, vol. 14, no. 8, pp. 1501–1521, 2012, doi: https://doi.org/10.3390/e14081501.
- [9] I. Rais, H. Mahmoudi, "The dimensioning of a compressed air motor dedicated to a compressed air storage system," *International Journal of Power Electronics and Drive Systems (IJPEDS)*, vol. 9, no. 1, pp. 73–79, Mar. 2018, doi: 10.11591/ijpeds.v9.i1.pp73-79.
- [10] I. Rais, H. Mahmoudi, "The control strategy for a hybrid wind-photovoltaic system with compressed air storage element," in *2016 International Conference on Electrical and Information Technologies (ICEIT)*, 2016, pp. 89–92, doi: 10.1109/EITech.2016.7519568.
- [11] I. Rais, H. Mahmoudi, "Study and dimensioning of the tanks dedicated to a compressed air storage system (CAES)," *International Journal of Electrical and Computer Engineering (IJECE)*, vol. 8, no. 4, pp. 2029–2037, Aug. 2018, doi: 10.11591/ijece.v8i4.pp2029-2037.
- [12] G. Dharmireddy, M. S., and S. Hanumanthakari, "A voltage controller in photo-voltaic system with battery storage for stand-alone applications," *International Journal of Power Electronics and Drive Systems (IJPEDS)*, vol. 2, no. 1, pp. 9–18, Nov. 2011, doi: 10.11591/ijpeds.v2i1.127.
- [13] S. Lemofouet-Gatsi, "Investigation and optimisation of hybrid electricity storage systems based on compressed air and supercapacitors," *Academic and Research Output*, Ph.D. dissertation, EPFL, Lausanne, 2006.
- [14] V. Kokaew, S. M. Sharkh, and M. Moshrefi-Torbati, "Maximum power point tracking of a small-scale compressed air energy storage system," *IEEE Transactions on Industrial Electronics*, vol. 63, no. 2, pp. 985–994, Feb. 2016, doi: 10.1109/TIE.2015.2477344.
- [15] E. Bazdar, M. Sameti, F. Nasiri, and F. Haghighat, "Compressed air energy storage in integrated energy systems: A review," *Renewable and Sustainable Energy Reviews*, vol. 167, p. 112701, 2022, doi: 10.1016/j.rser.2022.112701.
- [16] C. Liu, X. Su, Z. Yin, Y. Sheng, X. Zhou, Y. Xu, X. Wang, and H. Chen, "Experimental study on the feasibility of isobaric compressed air energy storage as wind power side energy storage," *Applied Energy*, vol. 364, p. 123129, 2024, doi: 10.1016/j.apenergy.2024.123129.
- [17] I. Rais, H. Mahmoudi, and C. Ed-Dahmani, "The strategy of maximum efficiency point tracking (MEPT) for a pneumatic motor dedicated to an compressed air energy storage system (CAES)," in *2019 International Conference on Wireless Technologies, Embedded and Intelligent Systems (WITS)*, Apr. 2019, pp. 1–5, doi: 10.1109/WITS.2019.8723658.
- [18] G. Venkataramani, E. Ramakrishnan, M. R. Sharma, A. H. Bhaskaran, P. K. Dash, V. Ramalingam, and J. Wang, "Experimental investigation on small capacity compressed air energy storage towards efficient utilization of renewable sources," *Journal of Energy Storage*, vol. 20, pp. 364–370, Dec. 2018, doi: 10.1016/j.est.2018.10.018.




- [19] H. Lund and G. Salgi, "The role of compressed air energy storage (caes) in future sustainable energy systems," *Energy Conversion and Management*, vol. 50, no. 5, pp. 1172–1179, 2009, doi: 10.1016/j.enconman.2009.01.032
- [20] M. Gavran, M. Fruk, and G. Vujisi, "Pi controller for DC motor speed realized with Arduino and Simulink," in *2017 40th International Convention on Information and Communication Technology, Electronics and Microelectronics (MIPRO)*, 2017, pp. 1557–1561, doi: 10.23919/MIPRO.2017.7973669.
- [21] M. Chahabi Bushehri, S. M. Zolfaghari, M. Soltani, M. H. Nabat, and J. Nathwani, "A comprehensive study of a green hybrid multi-generation compressed air energy storage (CAES) system for sustainable cities: Energy, exergy, economic, exergoeconomic, and advanced exergy analysis," *Sustainable Cities and Society*, vol. 101, p. 105078, Feb. 2024, doi: 10.1016/j.scs.2023.105078.
- [22] A. H. Alami, "Experimental assessment of compressed air energy storage (CAES) system and buoyancy work energy storage (BWES) as cellular wind energy storage options," *Journal of Energy Storage*, vol. 1, pp. 38–43, Jun. 2015, doi: 10.1016/j.est.2015.05.004.
- [23] R. Huggins, "Fundamentals, Materials and Applications," in *Energy Storage*, 2nd ed., Stanford, USA: Springer Cham, 2016, ISBN: 978-3-319-21239-5, doi: 10.1007/978-3-319-21239-5.
- [24] H. Yu, S. Engelkemier, and E. Gener, "Process improvements and multi-objective optimization of compressed air energy storage (CAES) system," *Journal of Cleaner Production*, vol. 335, p. 130081, Feb. 2022, doi: 10.1016/j.jclepro.2021.130081.
- [25] E. Assareh and A. Ghafouri, "An innovative compressed air energy storage (CAES) using hydrogen energy integrated with geothermal and solar energy technologies: A comprehensive techno-economic analysis - different climate areas- using artificial intelligent (AI)," *International Journal of Hydrogen Energy*, vol. 48, no. 34, pp. 12600–12621, Apr. 2023, doi: 10.1016/j.ijhydene.2022.11.233.
- [26] S. Bashiri, Mousavi, M. Adib, M. Soltani, A. R. Razmi, and J. Nathwani, "Transient thermodynamic modeling and economic analysis of an adiabatic compressed air energy storage (A-CAES) based on cascade packed bed thermal energy storage with encapsulated phase change materials," *Energy Conversion and Management*, vol. 243, p. 114379, Sep. 2021, doi: 10.1016/j.enconman.2021.114379.
- [27] M. King, A. Jain, R. Bhakar, J. Mathur, and J. Wang, "Overview of current compressed air energy storage projects and analysis of the potential underground storage capacity in India and the UK," *Renewable and Sustainable Energy Reviews*, vol. 139, p. 110705, Apr. 2021, doi: 10.1016/j.rser.2021.110705.
- [28] S. M. Alirahmi, A. R. Razmi, and A. Arabkoohsar, "Comprehensive assessment and multi-objective optimization of a green concept based on a combination of hydrogen and compressed air energy storage (CAES) systems," *Renewable and Sustainable Energy Reviews*, vol. 142, p. 110850, May 2021, doi: 10.1016/j.rser.2021.110850.

BIOGRAPHIES OF AUTHORS






Ilham Rais    received her engineering degree in Electrical from University of Sultan Moulay Slimane in 2014, and Ph.D. degree in 2020 from University of Mohamed 5-Rabat, Morocco. Currently she is a Professional Trainer at the industrial specialized institute-Marrakech, Morocco. Her research interests in renewable energy conversion systems, electrical energy storage systems, and power electronics. She can be contacted at email: ilhamrais2010@gmail.com.



Chafik Ed-dahmani    received his engineering degree in mechatronics from University of Abdelmalek Essaadi in 2014, and Ph.D. degree from the University of Mohamed 5-Rabat, Morocco. Currently he is an assistant professor in National Graduate School of Arts and Crafts-Meknès, Morocco. His research interests in renewable energy system conversion, controlling power converters, and microgrids. He can be contacted at email: c.eddahmani@umi.ac.ma.



Abdellah Benami    is a Full Professor at Engineering Sciences Department-Faculty of Sciences and Techniques since 12/2022. He has been the head of the physics department 2021-2023 and the head of the OTEA team since 2020. He earned his Ph.D. in Materials Science and Engineering from the National Autonomous University of Mexico in 2008. (UNAM). In recognition of his performance in the Ph.D. program, he received the Alfonso Caso Medal from UNAM in 2008. His primary research interests include photovoltaics, plasmonics, nanotechnology, metallic and semiconducting nanoparticles, and renewable energy. He can be contacted at email: a.benami@umi.ac.ma.